Sub-barrier fusion of ^{28,30}Si with ^{24,26}Mg

A. Morsad,* J. J. Kolata, R. J. Tighe, and X. J. Kong
Physics Department, University of Notre Dame, Notre Dame, Indiana 46556

E. F. Aguilera and J. J. Vega
Centro Nuclear, Instituto Nacional de Investigaciones Nucleares, Apartado Postal 18-1027, México, Distrito Federal, Mexico
(Received 6 November 1989)

Measurements of the fusion cross section of ^{28,30}Si + ^{24,26}Mg have been made for energies ranging from well below to above the Coulomb barrier. The fusion cross sections increased from about 40 μb at the lowest energy, to 400 mb or more at the highest energy measured. Surprisingly, a crossover in the excitation functions for ^{28,30}Si + ^{24}Mg is observed at the lowest sub-barrier energies. The data could not be reproduced by either a one-dimensional tunneling calculation or an approximate coupled-channels calculation within the constant coupling scheme. However, the use of an exact coupled-channels code, together with incoming-wave boundary conditions, led to good agreement between the calculated and measured fusion cross sections.

I. INTRODUCTION

The study of reactions between medium-heavy nuclei below the barrier provides a method to test the nuclear potential on the inner side of the interaction barrier. In addition, it might in this way be possible to gain information on the influence of nuclear structure upon the behavior of nuclear matter and the nuclear reaction dynamics, especially for those energies where penetrability effects are important. Thus, the study of heavy ion fusion reactions at energies well below the *s*-wave interaction barrier has attracted considerable theoretical and experimental interest. For a large variety of systems studied, the sub-barrier fusion cross section has been observed to present an unexpected enhancement, as compared with conventional models of tunneling through a one-dimensional potential barrier, which successfully describe fusion above the Coulomb barrier. Several attempts have been made to account for this sub-barrier fusion enhancement, from which it has become clear that inclusion of additional degrees of freedom besides the relative separation between the two nuclei allows for a better comprehension of the underlying physical process governing the cold dinuclear system. A detailed review on this subject can be found in Ref. 1. Among the theoretical approaches that have been put forward in this respect, we can mention models based on zero point fluctuations,[2] neck formation between reactants,[3] and static deformations of the nuclei involved.[4] Coupling of inelastic and/or transfer channels (especially those with positive Q value) to the fusion channel may also play an important role in the enhancement of the sub-barrier fusion cross section.[5] In spite of all the theoretical and the experimental effort, however, the precise mechanism leading to sub-barrier fusion cross-section enhancement in particular systems is still not fully understood. In order to further the understanding of the theoretical and the experimental aspects of this open question, it is necessary to extend sub-barrier fusion studies to other systems. It is in this perspective that we undertook the study of sub-barrier fusion cross sections for the ^{28,30}Si + ^{24,26}Mg systems. These nuclei are known to possess strongly collective first excited states with considerable deformations.[6] It should thus be interesting to investigate the effects of coupling these states to the fusion channel.

The experimental procedure is described in the following section. In Sec. III, the data are presented and compared in a first stage to calculations of a one-dimensional barrier penetration model. Next, a simple coupled-channel calculation performed using the approximate code[7] CCFUS is discussed, and finally full coupled-channel calculations are presented. Section IV contains the conclusions.

II. EXPERIMENTAL METHOD

The experiments were performed using ^{28,30}Si beams provided by the three-stage tandem Van de Graaf accelerator at the University of Notre Dame. The beam energy ranged from 46 to 66 MeV, in steps of 1 MeV. The ^{24}Mg and ^{26}Mg targets consisted of self-supporting metallic Mg foils that were isotopically enriched to 99.55% in the corresponding isotope. In order to verify the purity of the targets, α particles of incident energy $E_{\rm lab}=7.15$ MeV were elastically scattered at $\theta_{\rm lab}=45°$ and detected at the focal plane of a magnetic spectrograph. No contaminants other than a small amount of C and O were observed by this method. The thicknesses (128 μg/cm^2 for ^{24}Mg, 430 μg/cm^2 for ^{26}Mg), determined by measuring the energy loss of α particles from an ^{241}Am source, are estimated to be accurate to $\pm 10\%$.

The evaporation residues (ER) from fusion are emitted in a narrow cone within a few degrees around the beam axis, and their cross section is relatively small at energies below the barrier. Therefore, direct detection of residues becomes difficult in the presence of a large background arising from slit scattering and other similar types of events. To accomplish the separation, the evaporation

residues emerging from the target were deflected out of the direct beam by means of an electrostatic deflector. The value of the potential applied to the electrode plates was selected so as to maximize the yield from each target. The separated residues were then identified in a time-of-flight (TOF) and energy spectrometer, which consisted of a microchannel plate and a silicon surface barrier detector (SSB) which together defined a 1 m flight path. The whole apparatus (TOF arm, electrostatic deflector, and target chamber) was rigidly attached and designed to rotate as a unit, making it possible to measure the angular distribution over $\pm 10°$ with respect to the beam. A more complete and detailed report on this spectrometer will be the subject of a future publication. As can be seen in Fig. 1, the yield of ER can be obtained, essentially free of background, from the time of flight versus energy spectrum, which shows three well-separated islands of events. The lowest corresponds to the ER from Si+Mg reactions, while the two small groups in the middle are due to fusion of Si on carbon and oxygen in the target.

The transmission probability of the ER through the recoil velocity spectrometer was determined empirically by elastic scattering of ions of similar atomic and mass numbers, and kinetic energy. To accomplish this, we measured Rutherford scattering of ^{58}Ni ions on the magnesium targets at a laboratory energy $E=72$ MeV. We define the transmission probability as the ratio of the number of particles detected at the SSB detector to that initially traveling within the solid angle determined by the entrance slit of the TOF arm. Four silicon surface-barrier detector monitors placed inside of the target chamber symmetrically at 15° with respect to the beam axis gave a precise determination of the beam position on the target, as well as the product of the number of incident particles times the target thickness. This provided the absolute normalization for all cross sections. The experimental value of the transmission probability, $T=0.70\pm0.04$, was theoretically confirmed by a calculation using a Monte Carlo code. It has also been checked experimentally by additional measurements of sub-barrier fusion in the ^{32}S+^{24}Mg system, which has been previously studied by Berkowitz *et al.*[8] Excellent agreement is observed between the two data sets, as illustrated in Fig. 2, except at the very lowest energies where background events may become important.

Excitation functions for all systems were measured at

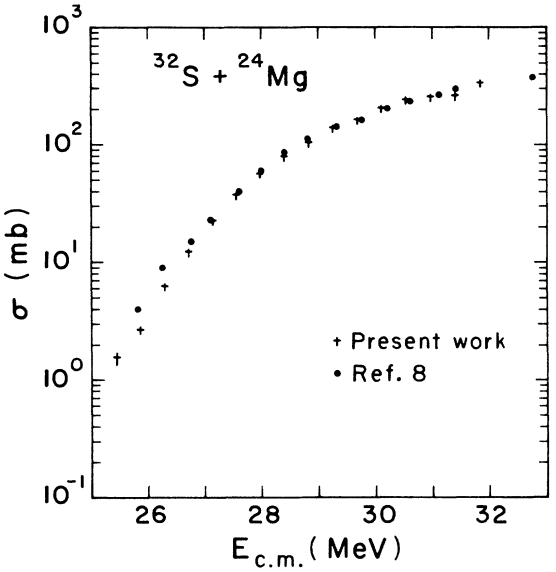

FIG. 2. Comparison between the total fusion excitation function of the ^{32}S+^{24}Mg system, obtained in the present work and in Ref. 8.

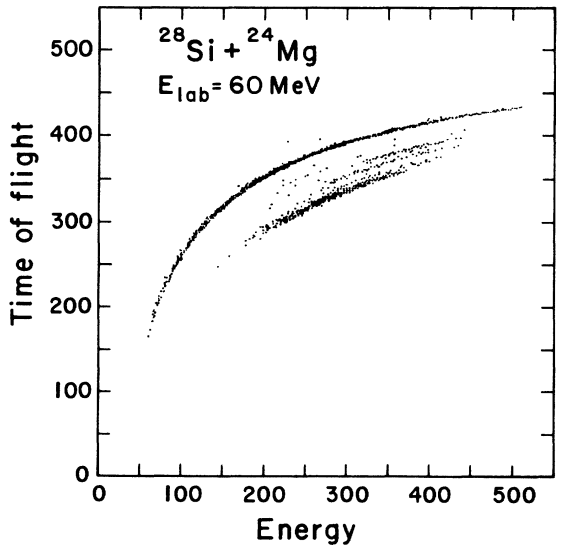

FIG. 1. The TOF/energy spectra for ^{28}Si+^{24}Mg at $\theta_{lab}=3°$ and $E_{lab}=60$ MeV. For details see the text.

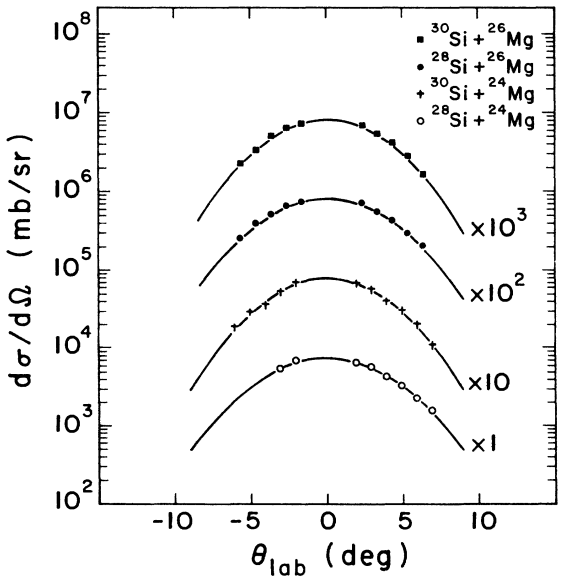

FIG. 3. Angular distributions of Si+Mg systems at $E_{lab}=60$ MeV, and the corresponding Gaussian fit (solid curve).

TABLE I. Total fusion cross sections for Si + Mg systems.

System	$E_{c.m}$ (MeV)	σ_{fus} (mb)	System	$E_{c.m}$ (MeV)	σ_{fus} (mb)
$^{28}Si+^{24}Mg$	20.9	0.078(25)	$^{28}Si+^{26}Mg$	21.7	0.13(2)
	21.4	0.21(41)		22.2	0.39(8)
	21.8	0.45(89)		22.6	1.08(12)
	22.3	1.10(18)		23.0	2.00(20)
	22.8	2.18(25)		23.6	5.00(41)
	23.2	6.13(52)		23.9	11.8(9)
	23.7	13.4(12)		24.3	21.9(18)
	24.1	25.9(18)		24.7	33.5(25)
	24.6	41.5(30)		25.1	52.6(36)
	25.1	67.2(46)		25.5	79.8(61)
	25.5	87.3(61)		25.9	107.3(77)
	25.9	115.6(81)		26.4	129.3(89)
	26.4	144(10)		26.9	170(12)
	26.9	186(13)		27.3	204(14)
	27.3	215(15)		27.7	240(17)
	27.8	223(16)		28.2	264(18)
	28.2	253(18)		28.6	295(20)
	28.7	292(20)		29.1	310(21)
	29.2	352(23)		29.6	348(24)
	29.6	381(26)		30.0	349(23)
	30.1	423(29)			
$^{30}Si+^{24}Mg$	21.1	0.073(42)	$^{30}Si+^{26}Mg$	21.0	0.042(30)
	21.5	0.24(6)		21.4	0.12(2)
	21.9	0.76(11)		21.8	0.35(4)
	22.4	2.12(22)		22.2	0.69(10)
	22.8	5.72(50)		22.7	1.61(15)
	23.2	12.2(9)		23.2	4.05(31)
	23.7	23.0(16)		23.6	9.68(93)
	24.1	41.4(29)		24.0	19.6(16)
	24.5	62.8(45)		24.3	36.0(29)
	25.0	91.2(65)		24.6	49.8(37)
	25.4	116.1(82)		25.1	69.2(50)
	25.9	145(10)		25.5	99.8(71)
	26.3	179(13)		25.9	128.4(89)
	26.7	198(14)		26.3	161(11)
	27.2	250(18)		26.8	199(13)
	27.6	278(20)		27.2	245(17)
	28.1	307(23)		27.6	289(20)
	28.5	332(24)		28.1	320(22)
				28.5	358(24)
				29.0	390(27)
				29.4	418(29)

an angle of $\theta_{lab}=3°$. In order to convert this single angle excitation function into a total fusion yield, ER angular distributions were measured at a laboratory bombarding energy of $E=60$ MeV. Since the shape of the ER angular distribution does not change substantially with incident energy, we can use the integration of the measured angular distribution at this energy to deduce the absolute cross sections at other energies. To do this, the angular distributions were fitted with a Gaussian function, and then integrated from 0° to 20°. That this upper limit of the integration is reasonable is illustrated in Fig. 3, which shows angular distributions measured for the four systems. Note that both left and right measurements were taken to ensure precise determination of the beam axis. Beam energy losses in the targets were corrected for by an iterative procedure, taking into account the slopes of the excitation function. At each step, corrected beam energies were obtained by weighting the energies from the previous step by the experimental fusion cross section, and averaging over the energy loss in the target. This process was repeated until self-consistent results were obtained.

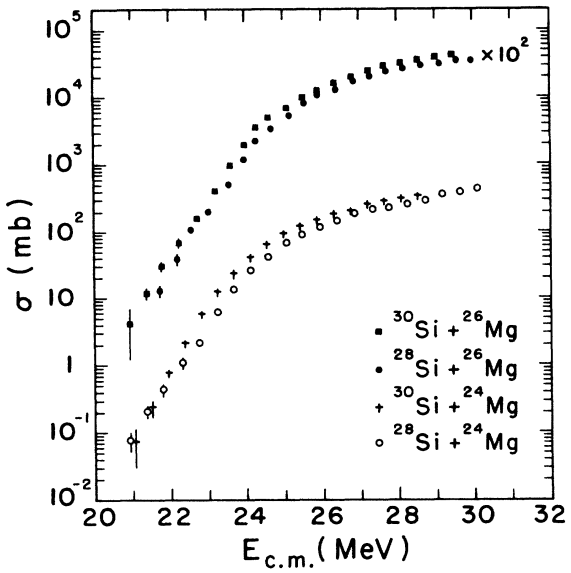

FIG. 4. Fusion excitation functions for the Si + Mg systems.

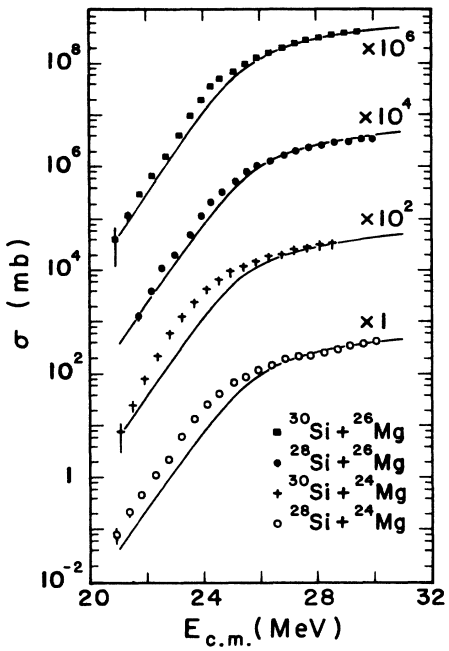

FIG. 5. The fusion excitation functions compared with the one-dimensional barrier penetration model calculations (solid curve).

III. RESULTS AND DISCUSSION

The experimental data are tabulated in Table I. Systematic errors of the order of 8% in the absolute yield, dominated by the uncertainty in the transmission of the spectrometer and the integration of the angular distributions, are estimated. The excitation functions are shown in Fig. 4. The measured cross sections span almost 4 orders of magnitude. For all systems they rise from approximately 40 μb at low energies and flatten out at about 300 mb at the highest energies. The excitation functions of the ^{28}Si + ^{26}Mg and ^{30}Si + ^{26}Mg systems have approximately the same shape over all the energy range, while, surprisingly, the ^{28,30}Si + ^{24}Mg excitation functions cross over each other at the lowest sub-barrier energies despite the lower fusion barrier for the latter system.

In a first attempt to understand the sub-barrier fusion in these systems, we compared our data with the predictions of a one dimensional tunneling model using the non-coupling mode of the code CCFUS.[7] The potential used in this calculation consisted of a sum of the Coulomb potential for two point charges, plus a centrifugal term and real nuclear potential having a Woods-Saxon shape. The Schrödinger equation is then solved assuming a black nucleus, so there are no reflections from the nuclear interior, and the fusion cross section is computed from Wong's formula:[9]

$$\sigma_{\text{fus}} = (R_b^2/2E_{\text{c.m.}})\hbar\omega \ln\{1+\exp[(2\pi/\hbar\omega)(E_{\text{c.m.}} - V_b)]\} \quad (1)$$

Here, R_b, V_b, and $\hbar\omega$ are the radius, height, and curvature of the barrier, respectively. The depth of the real part of the nuclear potential was adjusted in order to fit the data at high energy. The barrier parameters obtained from these calculations are listed in Table II, together with the corresponding values from the systematics established by Vaz *et al.*[3] Good agreement between the experimental and systematic barrier parameters is obtained. Figure 5 presents the results of this calculation compared with the experimental data. At sub-barrier energies, large enhancement are observed in the case of the ^{24}Mg systems, while enhancement is much less important (though still observable) for the ^{26}Mg systems. One may

TABLE II. Barrier parameters deduced from this work, and predictions from the systematics of Ref. 3.

System	This work V_b (MeV)	This work R_b (fm)	This work $\hbar\omega$ (MeV)	Systematics V_b (MeV)	Systematics R_b (fm)
^{28}Si + ^{24}Mg	25.1	8.93	3.49	25.0	8.91
^{30}Si + ^{24}Mg	24.8	9.05	3.40	24.7	9.02
^{28}Si + ^{26}Mg	25.0	8.95	3.39	24.6	9.03
^{30}Si + ^{26}Mg	24.8	9.05	3.29	24.4	9.14

TABLE III. Deformation parameters used in the coupled-channels calculations. The same deformation lengths were used in both CCFUS and PTOLEMY. The quadrupole deformations β_2 were determined from measured quadrupole moments (Ref. 6). The $B(E2)$ values were obtained from appropriately weighted individual $B(E2)$ values as given in Ref. 15.

Nucleus	J^π	E_x (MeV)	$B(E2)\uparrow$ (e^2b^2)	Q_2^+ (e fm^2)	$\beta_2 R$	β_4
^{24}Mg	2^+	1.37	0.0432(12)	−18(2)	1.81	
^{26}Mg	2^+	1.81	0.0305(13)	−13(3)	1.27	
^{28}Si	2^+	1.78	−0.0326(12)	+16(3)	−1.31	
	4^+	4.62				0.15
^{30}Si	2^+	2.24	0.0215(10)	−9(4)	0.72	

speculate that this difference is due to the relatively large prolate quadrupole deformation of the ^{24}Mg nucleus.

The above results clearly indicate that the present data cannot be described by a one-dimensional model. We are then naturally led to try to take into account the coupling to other degrees of freedom, such as the excitation of low-lying states of the projectile and target. To include these inelastic channels, we performed coupled-channels calculations within the constant coupling scheme, using a modified version of the program CCFUS,[10] which allows for a static rotor description. It was assumed for the purposes of this calculation that the Mg and Si nuclei possess a static deformation. The potential, and in particular the depth of its nuclear part, is otherwise the same as that used in the one-dimensional calculation. The deformation parameters, listed in Table III, were extracted from measured static quadrupole moments,[6] and it was assumed in these calculations that the ^{28}Si nucleus has an oblate shape, while ^{30}Si, ^{26}Mg, and ^{24}Mg nuclei are prolate. The results of this calculation are compared with the data in Fig. 6. The calculations overpredict the enhancement by a substantial amount, which may be due either to the fact that this simplified model calculation neglects the excitation energy of the rotational states, or to the breakdown of the sudden approximation in which it is assumed that the fusing nuclei do not rotate appreciably during the course of the interaction, so that the fusion probability may be calculated as a straightforward average over the results obtained for various target and projectile orientations.[10] Note that the relatively high excitation energy of the first excited state of these light, even-even nuclei (corresponding therefore to a high rotational frequency) makes rotation during the fusion interaction more likely.

In order to take into account the excitation energies of the projectile and target states, we have performed a full coupled-channels calculation using the code PTOLEMY,[11] with incoming wave boundary conditions. This technique has been used successfully by Landowne and Pieper[12] for the ^{58}Ni+^{58}Ni reaction. The set of coupled equations given by

$$[\partial/\partial r + K_b^2(r)]U_b(r) = 2\mu/\hbar^2 \Sigma_a V_{ba}(r) U_a(r) , \quad (2)$$

where μ is the reduced mass, $K_b(r)$ is the local wave number, and $V_{ba}(r)$ is the coupling interaction, is solved by imposing an incoming wave boundary condition of the form suggested by Rawitscher:[13]

$$U_b(r) \propto [1/K_b(r)] \exp\left[-i \int_{R_b} K_b(r')dr'\right] . \quad (3)$$

Here, R_b is the boundary radius taken to be inside the Coulomb barrier. This boundary condition ensures that any flux penetrating the barrier is not reflected back to a surface mode and may therefore be ascribed to fusion. The ER cross section is then determined as the difference

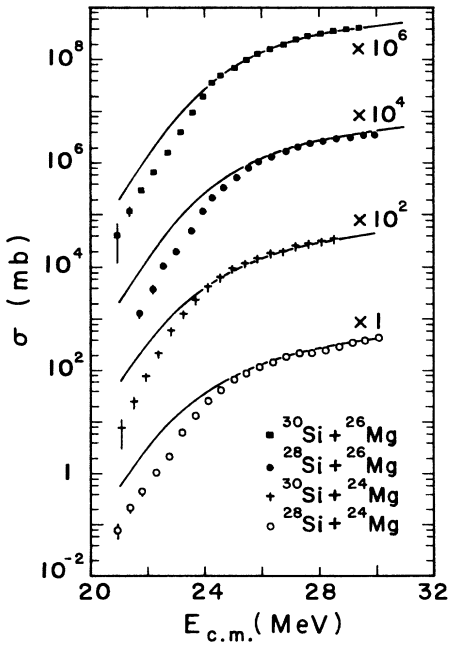

FIG. 6. The fusion excitation functions compared with CCFUS calculations using the static rotor description (solid curve).

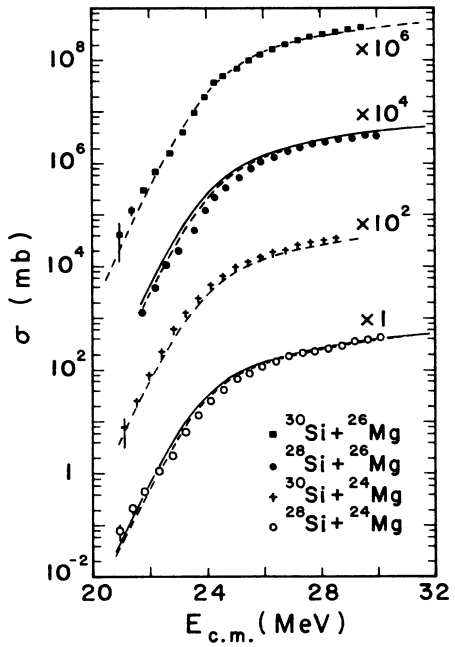

FIG. 7. Comparison of the experimental total fusion cross sections with PTOLEMY predictions. The dashed curve corresponds to coupling of the 2^+ excited states of target and projectile, while the solid curves correspond to the inclusion of the 4^+ state of ^{28}Si.

between the total reaction cross section and the total cross section in the excited channels. We used this approach to carry out coupled-channels calculations for the four systems. No transfer channel was included in the coupling scheme; only excitation of low-lying inelastic states was considered. A Wood-Saxon potential having a real depth $V_0=37$ MeV, a radius $r_0=1.18$ fm, and a diffuseness $a_0=0.63$ fm was used. The boundary radius was set inside the barrier at $R_b=6.7$ fm. Altering this radius around its nominal value has only a very small effect on the result. The deformation parameters and electromagnetic transition strengths used in the calculation are listed in Table III, and the results are compared with the experimental data in Fig. 7. We first considered the coupling of the first 2^+ excited states of the projectile and target (dashed curve). The magnitude of the cross section is well reproduced for all systems, except for the ^{28}Si+^{26}Mg system where the calculation slightly overpredicts the data. The solid curve shows the effect of the additional coupling of the 4^+ excited state in ^{28}Si ($E_x=4.62$ MeV), which is known[14] to have relatively large hexadecapole deformation ($\beta_4=0.15$). This increases the fusion cross section, while inclusion of the 4^+(4.62 MeV) to 2^+(1.78 MeV) transition, and the reorientation effect in ^{28}Si, lead to insignificant changes.

The fact that these calculations (including only the first excited states) account for essentially all of the enhancement observed over the one-dimensional barrier penetration model, and that the ^{24}Mg systems exhibit much more enhancement when compared with the ^{26}Mg systems, suggest that this difference is due to the large prolate quadrupole deformation of ^{24}Mg as we suggested above. Considering the fact that no free parameter was allowed in these model calculations we can conclude that, within this coupled-channels framework, the spectroscopic information from the literature provides a remarkably good description of the data. Furthermore, it appears unlikely that transfer reactions have a very important role to play in the fusion of the systems we have investigated, since inclusion of coupling to transfer channels can only increase the predicted yield.

Finally, despite the excellent overall agreement between data and prediction, some possibly interesting discrepancies still remain. In particular, the two systems involving ^{28}Si are both overpredicted in a region between the barrier and the far sub-barrier energies. While it is possible that this is an artifice of the data generated by an unknown systematic error in our relative normalization procedure, all of these data were taken at the same time with the same experimental setup. Furthermore, we observe no such discrepancies in the comparison with the data of Ref. 8, except for the small difference at the furthest sub-barrier energies which may be attributed to background subtraction problems at a level of a few hundreds of microbarns. Thus, the observed discrepancy in the near-barrier regime is very likely to be a real effect. In this regard, it is perhaps instructive to compare the one-dimensional tunneling calculations (Fig. 5) with the full coupled-channels result (Fig. 7) for the various systems. Note that the former accurately predict both the far sub-barrier yield (except possibly for ^{28}Si+^{24}Mg) and the above-barrier cross section, but fail in the intermediate energy regime. The effect of channel-coupling is primarily to boost the yield in the near-barrier region, and this results in excellent predictions for ^{30}Si+^{26}Mg, and especially for ^{30}Si+^{24}Mg where the near-barrier enhancement is particularly obvious. On the other hand, the predictions for the systems involving ^{28}Si are not as good, possibly suggesting the need to couple other surface-peaked quasielastic channels in these cases. Finally, we note that the surprising crossover of the ^{28,30}Si+^{24}Mg excitation functions is perhaps qualitatively reproduced by the coupled-channels calculations, which predict more sub-barrier enhancement for the former system (compare Figs. 5 and 7). However, it must also be noted that the predicted excitation functions do not actually cross over each other, so that a quantitative understanding of this phenomenon has not been achieved.

IV. CONCLUSIONS

We have obtained fusion excitation functions around and well below the barrier for the reactions ^{28,30}Si+^{24,26}Mg, using an electrostatic deflector in conjunction with a TOF/energy telescope. The measured fusion cross sections covered 4 orders of magnitude from 40 μb to 400 mb. The experimental data show enhancements when compared with calculations based on a one-dimensional tunneling model, with the ^{24}Mg systems exhibiting the most enhancement. Coupled-channel calculations within the constant coupling scheme, and using a static rotor description, overpredict the data. A full

coupled-channels calculation with incoming wave boundary conditions was carried out, and good agreement was achieved when the first 2^+ states of the projectile and target were included. However, some discrepancies in the middle energy range still remain for the systems involving ^{28}Si. The explanation of this relative suppression of the fusion yield at near-barrier energies may provide some useful insights into nuclear reaction dynamics in the "nuclear exosphere," i.e., where cold nuclear matter is very slightly overlapping.

ACKNOWLEDGMENTS

We would like to thank Dr. S. Landowne for fruitful discussions on the coupled-channels calculations. We also express our thanks to R. Kryger and S. Dixit for their help in data acquisition. This work was supported by the U.S. National Science Foundation under Contract Nos. INT 88-03658 and PHY 88-03035 and by Consejo Nacional de Ciéncia (Mexico) under Contract No. 140105 0102-139.

*Present address: Centre de Recherches Nucleaires and Universite Louis Pasteur, 67037 Strasbourg CEDEX, France.

[1]M. Beckerman, Phys. Rep. **129**, 145 (1985); M. Beckerman, Rep. Prog. Phys. **51**, 1047 (1988).

[2]W. Reisdorf, F. P. Hessberger, K. D. Hildenbrand, S. Hofman, G. Munzenberg, K. H. Schmidt, J. H. R. Schneider, W. F. W. Schneider, K. Summerer, G. Wirth, J. V. Kratz, and K. Schlitt, Phys. Rev. Lett. **49**, 1811 (1982).

[3]L. C. Vaz, J. M. Alexander, and G. R. Satchler, Phys. Rep. **69**, 373 (1981).

[4]R. G. Stokstad, W. Reisdorf, K. D. Hildenbrand, J. V. Kratz, G. Wirth, R. Lucas, and J. Poitou, Z. Phys. A **295**, 269 (1980); R. G. Stokstad and E. E. Gross, Phys. Rev. C **23**, 281 (1981).

[5]C. H. Dasso, S. Landowne, and A. Winther, Nucl. Phys. **A405**, 381 (1983); R. A. Broglia, C. H. Dasso, S. Landowne, and G. Pollarolo, Phys. Lett. **133B**, 34 (1983).

[6]R. H. Spear, Phys. Rep. **73**, 369 (1981).

[7]C. H. Dasso and S. Landowne, Phys. Lett. B **183**, 141 (1987).

[8]G. M. Berkowitz, P. Braun-Munzinger, J. S. Karp, R. H. Freifelder, T. R. Renner, and H. W. Wilschut, Phys. Rev. C **28**, 667 (1983).

[9]C. Y. Wong, Phys. Rev. Lett. **31**, 766 (1973).

[10]S. Landowne, private communication.

[11]D. H. Gloeckner, M. H. Macfarlane, and S. C. Pieper, Argonne National Laboratory Report No. ANL-76-11, 1978 (unpublished); M. Rhoades-Brown, M. H. Macfarlane, and S. C. Pieper, Phys. Rev. C **21**, 2417 (1980); **21**, 2436 (1980).

[12]S. Landowne and S. C. Pieper, Phys. Rev. C **29**, 1352 (1984).

[13]G. H. Rawitscher, Nucl. Phys. **85**, 337 (1966).

[14]H. Rebel and G. W. Schweimer, Z. Phys. **262**, 59 (1973).

[15]S. Raman, C. H. Malarkey, W. T. Milner, C. W. Nestor, and P. H. Stelson, At. Data Nucl. Data Tables **36**, 1 (1987).